Monthly Notices of the ROYAL ASTRONOMICAL SOCIETY

MNRAS **504,** 1545–1554 (2021)
Advance Access publication 2021 April 05
doi:10.1093/mnras/stab943

Three ultraluminous X-ray sources hosted by globular clusters in NGC 1316

Kristen C. Dage,[1,2★] Arunav Kundu,[3] Erica Thygesen,[4] Arash Bahramian,[5] Daryl Haggard,[1,2] Jimmy A. Irwin,[6] Thomas J. Maccarone,[7] Sneha Nair,[1] Mark B. Peacock,[3] Jay Strader[4] and Stephen E. Zepf[4]

[1]Department of Physics, McGill University, 3600 University Street, Montréal, QC H3A 2T8, Canada
[2]McGill Space Institute, McGill University, 3550 University Street, Montréal, QC H3A 2A7, Canada
[3]Eureka Scientific, Inc., 2452 Delmer Street, Suite 100, Oakland, CA 94602, USA
[4]Department of Physics and Astronomy, Michigan State University, East Lansing, MI 48824, USA
[5]International Centre for Radio Astronomy Research – Curtin University, GPO Box U1987, Perth, WA 6845, Australia
[6]Department of Physics and Astronomy, University of Alabama, Box 870324, Tuscaloosa, AL 35487, USA
[7]Department of Physics, Texas Tech University, Box 41051, Science Building, Lubbock, TX 79409-1051, USA

Accepted 2021 March 29. Received 2021 March 26; in original form 2021 February 19

ABSTRACT

We have identified three ultraluminous X-ray sources (ULXs) hosted by globular clusters (GCs) within NGC 1316's stellar system. These discoveries bring the total number of known ULXs in GCs up to 20. We find that the X-ray spectra of the three new sources do not deviate from the established pattern of spectral behaviour of the other known GC ULXs. The consistency of the X-ray spectral behaviour for these sources points to multiple paths of formation and evolution mechanisms for these rare and unique sources. Using the now larger sample of GC ULXs, we compare the optical properties of the entire known population of GC ULXs to other GCs across five galaxies and find that the properties of clusters that host ULXs are quite different from the typical clusters. Lastly, any trend of GC ULXs being preferentially hosted by metal-rich clusters is not strongly significant in this sample.

Key words: globular clusters: general – X-rays: binaries.

1 INTRODUCTION

Ultraluminous X-ray sources (ULXs) are off-nuclear X-ray point sources with luminosities exceeding the Eddington limit for a 10 solar mass black hole (BH), typically $\gtrsim 10^{39}$ erg s^{-1}. Most ULXs tend to occur in young, star-forming regions of spiral galaxies, and a handful have identified neutron star (NS) accretors, identified by pulsations, possibly with high magnetic fields (Bachetti et al. 2014; Brightman et al. 2018; Hu, Ueda & Enoto 2021, and references therein). Statistical evidence for such sources in elliptical galaxies is poor (Irwin, Bregman & Athey 2004), but starting with the source XMMU J122939.7+075333 in the globular cluster RZ2109 in the galaxy NGC 4472 (Maccarone et al. 2007), a growing number of globular cluster (GC) ULXs in elliptical galaxies have been discovered. With the GC association, the problem of distinguishing between background active galactic nuclei (AGNs) projected against a galaxy and bona fide members of the galaxies is ameliorated, and secure identifications of ULXs in these older populations can be made.

For these GC ULXs, BH accretors offer the most likely explanation. Since these ULXs exist in crowded, older stellar populations, the only remaining donor stars are low mass and hydrogen deficient. In these dense stellar environments, binaries are formed dynamically. Given the number of differences between the old, crowded GC environment and the young regions where NS ULXs have been identified, this implies the accretion phenomena and compact objects of GC ULXs may be fundamentally different from the physics behind the younger NS ULXs [see also theoretical work such as Wiktorowicz et al. (2021), which suggests that the physics powering ULXs in young (<100 Myr) environments is vastly different from the physics in environments >2 Gyr].

Identifying these BH candidates in extragalactic GCs is exciting because, while many studies have identified BHs and BH candidates in Galactic GCs (Strader et al. 2012a; Chomiuk et al. 2013; Miller-Jones et al. 2015; Giesers et al. 2018, 2019; Shishkovsky et al. 2018), the Milky Way is home to fewer than 300 GCs. By contrast, the total number of clusters in even a single elliptical galaxy can be larger than ∼100 the number in the Milky Way, offering tens of thousands more clusters for study. This allows for broader statistical studies of the nature of BH-hosting clusters than can be accomplished in the Milky Way.

The nature and number of these sources have important implications for the progenitors of the BH–BH binary mergers detected by the Laser Interferometer Gravitational-Wave Observatory (LIGO), as GCs are a likely birthplace of these sources (Abbott et al. 2016; Rodriguez et al. 2019). BHs are also important for understanding cluster evolution (Giersz et al. 2019; Kremer et al. 2019), as BHs may play an important role in the cluster dynamics (Ye et al. 2020). This marks a dramatic shift from early theoretical work, which predicted that while BHs certainly formed in GCs, they would be thrown out of the cluster due to either natal kicks or gravitational interactions (e.g. Spitzer 1969).

★ E-mail: kristen.dage@mail.mcgill.ca

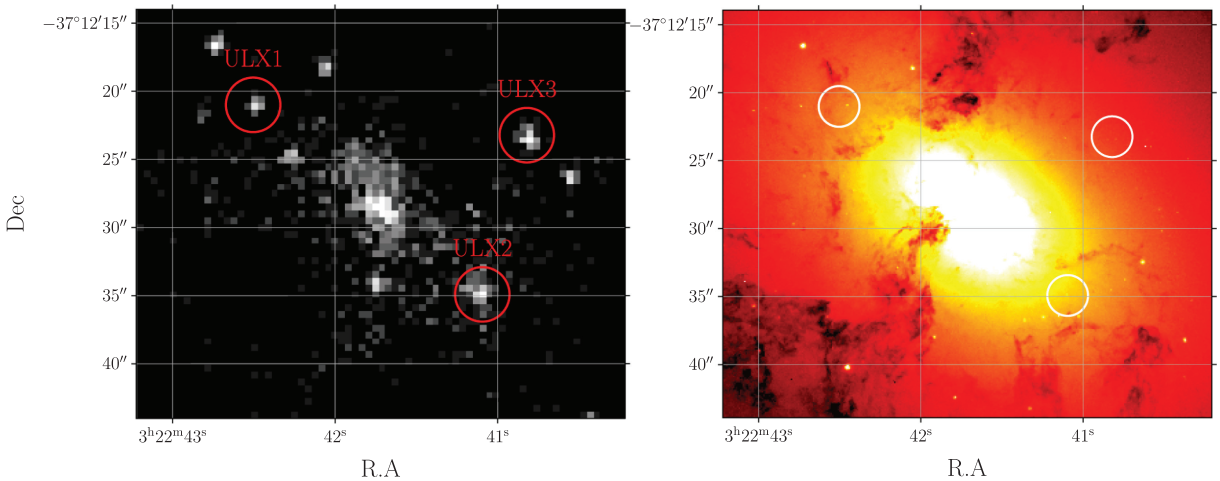

Figure 1. Left: X-ray image of NGC 1316 (ObsID 20341) with positions of the three GC ULXs overlaid. Right: *HST F475W* (Sloan *g* band) image of NGC 1316 with the GC ULXs overlaid.

Table 1. Left-hand columns: *Chandra* observations of NGC 1316, all observations are ACIS-S. Right-hand columns: *HST* observations for *g* and *z* (AB mag) observations.

ObsID (*Chandra*)	Date	Exposure (ks)	ObsID (*HST*)	Date	Filter	Exposure (s)
2022	2001-04-17	30	j90x01020	2005-02-16	*F475W* (*g*)	760
20340	2019-04-10	45	j90x01010	2005-02-16	*F850LP* (*z*)	1130
20341	2019-04-22	52				
22179	2019-04-17	39				
22180	2019-04-20	14				
22187	2019-04-25	53				

The first ULX associated with a GC was identified by Maccarone et al. (2007). The source displayed unusual short-term variability on the scale of hours, as well as luminous and broad [O III] emission lines, visible above the host cluster continuum (Zepf et al. 2008; Steele et al. 2011). Analysis by Peacock et al. (2012) measured a sizeable oxygen nebula in the system. Steele et al. (2014) placed limits on any excess hydrogen emission ([O III]/Hβ = 106) and identified a carbon–oxygen white dwarf as the very likely donor star of the system. The long-term X-ray and optical properties of the source were studied by Dage et al. (2018, 2019b), which showed that the X-ray luminosity varied by several orders of magnitude over 16 yr, and the optical luminosity of the line declined over a 7-yr period. Subsequent observations indicate that the optical luminosity has been rising for the last 2 yr, placing constraints on the size of the oxygen nebula (10^{-3} pc at minimum, but possibly up to 2 pc).

In 2010, two GC ULXs were identified in NGC 1399, the central galaxy in the Fornax Cluster. One of these showed short variability on the time-scales of hours, and was bright in X-rays until 2003, but has not been detected since (Shih et al. 2010). The other GC ULX did not show variability within an observation, but showed narrow [O III] and [N II] emission lines above the host cluster continuum (Irwin et al. 2010).

Maccarone et al. (2011) discovered a second GC ULX hosted by one of the NGC 4472's clusters, and Roberts et al. (2012) identified a GC ULX in an NGC 4649 cluster. Optical spectroscopy of the NGC 4649 cluster revealed no emission lines beyond the host cluster continuum, implying that not every GC ULX is host to optical emission. Irwin et al. (2016) discovered X-ray sources hosted by two GCs that flared above the Eddington limit on the time-scale of just minutes. Similar sources were also identified by Sivakoff, Sarazin & Jordán (2005).

Dage et al. (2019a) conducted the first ever large-scale, long-term X-ray analysis of GC ULXs in NGC 4472, NGC 4649, and NGC 1399, comparing the X-ray spectral properties of these and other sources. One of the major results of this work was that the two clusters that were known to exhibit optical emission lines showed markedly different X-ray behaviour than the rest of the sample, with lower best-fiting inner disc temperatures and spectral shapes uncorrelated with major changes in X-ray luminosity.

Seven more GC ULXs were identified by Dage et al. (2020), associated with the large GC population of M87. The X-ray spectra of these sources behaved like the larger GC ULX sample (and unlike the optical emission-line GC ULXs). A third source with significant short-term variability was identified. Lastly, it was shown that the ULXs were preferentially hosted by brighter (and hence, presumably, more massive) clusters, but did not show evidence for a correlation between the cluster colour and presence of a ULX.

In this work, we look to NGC 1316 to identify new GC ULX sources. NGC 1316 is a giant early-type galaxy that underwent a merger as recently as 1–3 Gyr ago (Goudfrooij et al. 2001a; see also work by Kleiner et al. 2021, for a discussion of the galaxy's history). Studies of the galaxy's GC system show that it is made up of two distinct populations of younger and older clusters (Goudfrooij et al. 2001b). Studies of the H I content of the galaxy give further agreement that NGC 1316 is the product of a merger of a lenticular and a spiral galaxy (Kleiner et al. 2021).

We use archival *Chandra* and *HST* data to identify three new GC ULXs in NGC 1316, and compare the X-ray spectral properties of the sources to the previously identified GC ULXs, as well as the optical properties of the host clusters. Section 2 describes the data and analysis techniques used for both optical and X-ray data reduction. Section 3 discusses the results of this work and compares

Table 2. X-ray coordinates of the three ULXs and lower X-ray luminosity sources coincident with candidate GCs. These sources have been identified in Kim & Fabbiano (2003), Swartz et al. (2004), and Allak et al. (2020). Sources marked with ^{o} were identified by Goudfrooij et al. (2001b), sources with † were identified by Jordán et al. (2015). X-ray luminosity estimates are based off of SRCFLUX calculations from ObsID 22187. Source counts and errors are based off of WAVDETECT measurements of ObsID 22187. CXOU J032238−371228 was only measured in the Vega magnitude system by Goudfrooij et al. (2001b), and hence there are no AB magnitudes to report.

Name	RA	Dec.	L_X estimate $\times 10^{39}$ erg s^{-1}	Counts 0.5−7.0 keV	z band (AB mag)	$g - z$
CXOU J032242.5−371222 (GCULX1) †	03:22:42.48	−37:12:21.15	1.39	112 ± 11	20.88	1.67
CXOU J032241.07−371235.3 (GCULX2) †	03:22:41.11	−37:12:34.73	1.05	61 ± 9	21.98	1.49
CXOU J032240.8−371224 (GCULX3)	03:22:40.82	−37:12:23.28	2.15	159 ± 16	23.10	0.94
CXOU J032244−371310 ^{o}	03:22:44.71	−37:13:10.07	0.15	9 ± 3	20.81	1.11
CXOU J032241−371304 ^{o} †	03:22:41.89	−37:13:04.49	0.33	17 ± 4	22.64	1.36
CXOU J032242−371258 ^{o}	03:22:42.43	−37:12:58.83	0.85	61 ± 8	22.37	1.72
CXOU J032240−371244 ^{o}	03:22:40.42	−37:12:44.51	0.13	16 ± 5	22.02	1.40
CXOU J032237−371251 ^{o}	03:22:37.69	−37:12:51.11	0.21	16 ± 4	18.19	1.27
CXOU J032238−371211 ^{o}	03:22:38.19	−37:12:11.58	0.12	9 ± 3	22.06	1.02
CXOU J032239−371148 ^{o} †	03:22:39.12	−37:11:48.00	0.70	64 ± 8	21.55	1.47
CXOU J032242−371218 ^{o}	03:22:42.06	−37:12:18.25	0.41	35 ± 7	18.55	1.40
CXOU J032242−371216 ^{o} †	03:22:42.73	−37:12:16.62	0.41	36 ± 6	18.16	1.24
CXOU J032242−371206 ^{o} †	03:22:42.60	−37:12:06.25	0.20	10 ± 3	22.40	0.99
CXOU J032242−371123 ^{o}	03:22:42.10	−37:11:23.92	0.42	47 ± 7	23.91	1.23
CXOU J032241−371117 ^{o} †	03:22:41.29	−37:11:17.13	0.30	19 ± 4	21.65	1.08
CXOU J032238−3712 †	03:22:38.78	−37:12:28.66	0.13	17 ± 4	N/A	N/A

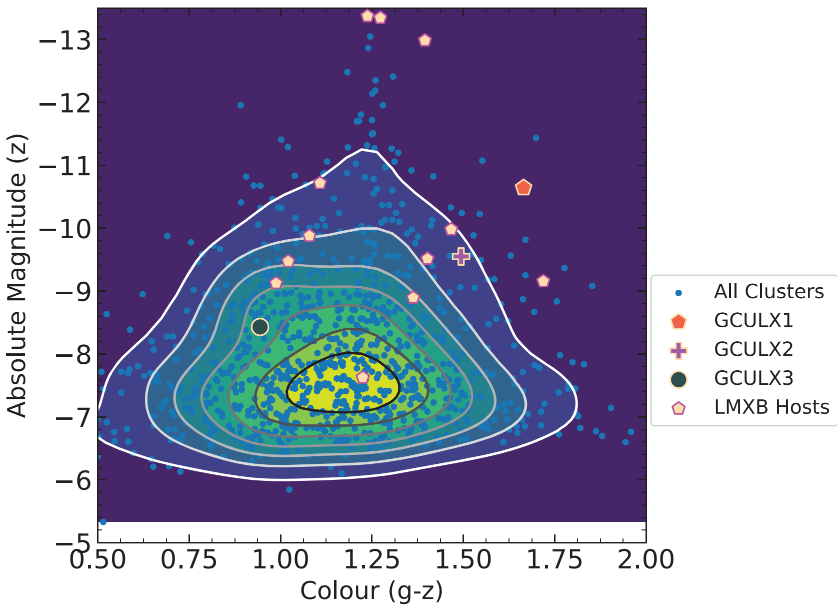

Figure 2. Colour and magnitude of the three GC ULXs in NGC 1316 compared to the overall population of GCs.

the X-ray and optical properties of the 20 known GC ULXs. Finally, the implications of this analysis are discussed in Section 4.

2 OBSERVATIONS AND ANALYSIS

We analysed archival X-ray and optical data of NGC 1316 to identify three ULXs hosted by GCs in this galaxy (see Fig. 1). The data are displayed in Table 1, and include six *Chandra* X-ray observations, with one taken in 2001 and five spread across a single month in 2019. We use *HST* observations in the *F475W* and *F850LP* filters (Sloan g and z bands in the AB magnitude system) to identify potential GC counterparts, as described in Section 2.2.

2.1 Identification of ULX sources

To identify the X-ray point source populations, we use the function WAVDETECT from CIAO on each X-ray image, which were cleaned and filtered of background flares, with the exposure map centred at 2.3 keV, and wavelet scales of 1.0, 2.0, 4.0, 8.0, and 16.0 pixels. We use an enclosed count fraction of 0.3, and significance threshold of 10^{-6}. This corresponds to about one false detection per chip, although the false detection will not have a flux corresponding to a ULX. We then estimate the fluxes of the identified sources by using the function SRCFLUX, assuming a fixed power law of $\Gamma = 1.7$, the typical power-law index for X-ray binaries, and fixed the hydrogen column density, N_H, to the line-of-sight density, 2.13×10^{20} cm^{-2}

Table 3. Total background subtracted counts in the 0.5–8.0 keV band and best-fitting spectral parameters for combined spectra of the three GC ULXs.

Source	Total counts (0.5–8.0 keV)	Power law Γ_{PL}	χ^2_ν/d.o.f.	*F*-test prob. (per cent)	diskbb kT_{in} (keV)	χ^2_ν/d.o.f.	*F*-test prob. (per cent)
GCULX1	272	1.4 (±0.3)	0.42/11	–	1.5 ($^{+0.7}_{-0.4}$)	0.62/11	–
GCULX2	613	1.8 (±0.1)	1.29/26	5	1.2 (±0.2)	1.08/26	53
GCULX3	484	1.6 (±0.1)	1.01/21	–	1.3 (±0.2)	0.87/21	–

Table 4. *Chandra* fit parameters and fluxes (0.5–8 keV) for spectral best-fitting single-component models, `tbabs*pegpwrlw` and `tbabs*diskbb` for NGC 1316 GCULX1. Hydrogen column density (N_H) frozen to 2.13 × 10^{20} cm^{-2}. All fluxes shown are unabsorbed in the 0.5–8 keV band. In ObsID 22180, GCULX1 has a background subtracted count rate of 8.84 × 10^{-4} counts s^{-1} in the 0.5–8 keV range. The upper limit was calculated using a fixed power-law index of Γ = 1.4.

ObsID (date)	NGC 1316 GCULX1 `tbabs*pegpwrlw` Γ	χ^2_ν/d.o.f.	PL flux (10^{-14} erg s^{-1} cm^{-2})	`tbabs*diskbb` T_{in} (keV)	Disc norm (10^{-4})	χ^2_ν/d.o.f.	Disc flux (10^{-14} erg s^{-1} cm^{-2})
2022 (2001-04-17)	1.3 (±0.4)	(44.36/51)	2.9 ($^{+1.2}_{-0.9}$)	1.7 ($^{+2.2}_{-0.6}$)	≤1.7	(44.44/51)	2.4 ($^{+1.3}_{-0.7}$)
20340 (2019-04-10)	1.2 (± 0.5)	(70.61/63)	1.7 (±0.6)	2.0 ($^{+4.5}_{-0.8}$)	≤0.5	(69.02/63)	1.5 (±0.6)
20341 (2019-04-22)	1.6 (±0.6)	(30.78/34)	1.3 (±0.5)	1.5 ($^{+1.8}_{-0.6}$)	≤1.1	(31.62/34)	1.1 (±0.5)
22179 (2019-04-17)	1.9 (±0.7)	(32.05/30)	1.2 (±0.5)	1.4($^{+2.3}_{-0.6}$)	≤1.3	(35.09/30)	1.0 (±0.5)
22180 (2019-04-20)	1.4	–	≤1.3	–	–	–	–
22187 (2019-04-25)	1.4 (± 0.4)	(47.22/60)	1.9 (±0.5)	1.6 ($^{+1.3}_{-0.5}$)	≤1.2	(47.74/60)	1.7 (±0.6)

(Dickey & Lockman 1990). We use the distance of 20.0 Mpc[1] to estimate the X-ray luminosity for all of the sources. This yields three unique X-ray point sources with luminosities near or exceeding the Eddington limit. While this analysis is only concerned with sources that have X-ray luminosities exceeding the Eddington limit for a 10 solar mass BH, it is worth noting that there are a number of less bright X-ray sources associated with GCs in the sample from Jordán et al. (2009).

2.2 *HST* analysis and globular cluster counterpart identification

We use catalogues of the GC population of NGC 1316 from Goudfrooij et al. (2001b) and Jordán et al. (20156) to identify three new ULXs hosted by GCs. Two ULX sources, GCULX1 and GCULX2, match to GC candidates in the Jordán et al. (2015) survey. GCULX3's optical counterpart, identified in Allak et al. (2020), also had characteristics typical of extragalactic GCs. We use DAOPHOT (Stetson 1987) to perform photometry on all three sources, as well as other known GCs in the field, using images that corresponds to the *g*, *z* bands, and found that GCULX3's colour and magnitude are typical for a GC. The ACS and WFC3 zero-points adopted from the *HST* ACS and WFC3 data handbook.[2]

We measure the half-light radius with BAOLAB (Larsen 1999) using the KING30 model convolved with a PSF made in TINY TIM (Krist, Hook & Stoehr 2011), and found the size of GCULX3 was on par with the GCs identified as having a 100 per cent probability of being a GC in Jordán et al. (2015).

The coordinates of the three GC ULX sources are listed in Table 2, along with their measured colour and magnitude in the AB system. The optical properties of the host clusters compared to the rest of the cluster population in the NGC 1316 are displayed in Fig. 2.

2.3 X-ray analysis

These sources were analysed in the same manner as Dage et al. (2019a, 2020), in order to compare the X-ray properties of all of the 20 identified GC ULXs to each other. The sources were extracted in each observation using CIAO, and the background regions were created by placing regions of a similar size to the source region near the source, but avoiding any nearby point sources. We use XSPEC (Arnaud 1996) to fit the spectra in the 0.5–8.0 keV band with single component models: `tbabs*diskbb` and `tbabs*pegpwrlw`. Any observation with greater than 100 counts is binned by 20, and any observation with fewer than 100 counts is binned by 1 and fit using the Cash statistic (Cash 1979). In ObsID 22180, both GCULX2 and GCULX3 have too few counts to extract a spectrum, and we estimate an upper limit using PIMMS. We use COMBINE_SPECTRA to combine all of the extracted spectra for each source (see Table 3 for the best-fitting values), but also fit each observation individually. The X-ray fits for each source can be found in Tables 4–6. The best-fitting power-law index of the combined spectra was used to estimate the upper limits for GCULX2 and GCULX3 in ObsID 22180. We also fit the two-component model `tbabs*(diskbb + pegpwrlw)` to the deep spectra, however, only GCULX2 could be fitted by the two-component model. We use *F*-test to determine whether the two-component model was statistically a better fit than either single component model, but given that the *F*-test null hypothesis probability was high for either case, this implies that the complexity of the two-component model is not justified. Since this is likely due to the source having many more counts than the other two sources, we do not report the values.

[1]The distance to the Fornax Cluster used in Dage et al. (2019a).
[2]https://www.stsci.edu/hst/documentation

Table 5. *Chandra* fit parameters and fluxes (0.5–8 keV) for spectral best-fitting single-component models, `tbabs*pegpwrlw` and `tbabs*diskbb` for NGC 1316 GCULX2. Hydrogen column density (N_H) frozen to 2.13 × 10^{20} cm^{-2}. All fluxes shown are unabsorbed in the 0.5–8 keV band.

NGC 1316 GCULX2							
	`tbabs*pegpwrlw`			`tbabs*diskbb`			
ObsID (date)	Γ	χ^2_ν/d.o.f.	PL flux (10^{-14} erg s^{-1} cm^{-2})	T_{in} (keV)	Disc norm (10^{-3})	χ^2_ν/d.o.f.	Disc flux (10^{-14} erg s^{-1} cm^{-2})
2022 (2001-04-17)	1.6 (±0.7)	0.362/3	3.3 ($^{+3.0}_{-1.3}$)	0.7 ($^{+1.6}_{-0.25}$)	≤3.7	0.23/3	1.7 ($^{+2.4}_{-0.5}$)
20340 (2019-04-10)	1.5 (±0.5)	1.139/61	2.2 (±0.6)	1.4 ($^{+0.9}_{-0.4}$)	≤0.2	0.9385/61	1.8 (±0.5)
20341 (2019-04-22)	1.4 (±0.6)	0.848/3	3.1 ($^{+1.2}_{-0.9}$)	1.2 ($^{+1.8}_{-0.4}$)	≤0.5	0.561/3	2.2 ($^{+1.3}_{-0.6}$)
22179 (2019-04-17)	2.2 (±0.6)	(65.04/52)	2.0 (±0.5)	0.9($^{+0.5}_{-0.3}$)	≤1.6	(69.92/52)	1.5 (±0.5)
22180 (2019-04-20)	1.9 (±0.8)	(38.26/29)	2.7 ($^{+1.2}_{-0.9}$)	1.1($^{+1.6}_{-0.4}$)	≤0.7	(38.15/29)	2.1 ($^{+1.2}_{-0.8}$)
22187 (2019-04-25)	1.7 (±0.4)	0.93/5	3.7 (±0.6)	1.2 ($^{+0.6}_{-0.3}$)	≤0.7	1.29/5	2.9 (±0.6)

Table 6. *Chandra* fit parameters and fluxes (0.5–8 keV) for spectral best-fitting single-component models, `tbabs*pegpwrlw` and `tbabs*diskbb` for NGC 1316 GCULX3. Hydrogen column density (N_H) frozen to 2.13 × 10^{20} cm^{-2}. All fluxes shown are unabsorbed in the 0.5–8 keV band. In ObsID 22180, the upper limit for GCULX3 was estimated using a background subtracted count rate of 9.58 × 10^{-4} counts s^{-1} in the 0.5–8 keV range.

NGC 1316 GCULX3							
	`tbabs*pegpwrlw`			`tbabs*diskbb`			
ObsID (date)	Γ	χ^2_ν/d.o.f.	PL flux (10^{-14} erg s^{-1} cm^{-2})	T_{in} (keV)	Disk norm (10^{-3})	χ^2_ν/d.o.f.	Disc flux (10^{-14} erg s^{-1} cm^{-2})
2022 (2001-04-17)	1.2 (±0.5)	0.08/2	1.7 (±0.6)	0.8 ($^{+0.5}_{-0.3}$)	≤1.6	0.26/2	1.2 (±0.5)
20340 (2019-04-10)	1.7 (±0.5)	(46.78/48)	1.7 (±0.7)	1.2 ($^{+0.9}_{-0.4}$)	≤0.3	(47.78/48)	1.4 (±0.5)
20341 (2019-04-22)	1.6 (±0.5)	1.16/3	3.4 ($^{+1.2}_{-0.5}$)	1.1 ($^{+1.0}_{-0.3}$)	≤0.9	0.98/3	2.3 ($^{+1.1}_{-0.6}$)
22179 (2019-04-17)	1.6 (±0.6)	(34.44/51)	2.3 (±0.7)	1.4 ($^{+1.9}_{-0.3}$)	≤0.3	(34.48/51)	1.9 ($^{+0.8}_{-0.5}$)
22180 (2019-04-20)	1.6	–	≤1.7	–	–	–	–
22187 (2019-04-25)	1.2 (±0.5)	0.34/3	4.5 ($^{+1.4}_{-1.1}$)	2.1 ($^{+2.1}_{-0.9}$)	≤0.1	0.422/3	3.7 ($^{+2.1}_{-1.1}$)

Lastly, we extract background-subtracted light curves using DMEXTRACT and find no evidence of strong variability (see also analysis by Allak et al. 2020, for lack of variability in GCULX3). This is typical for most GCULXs, currently only three of them show strong variability (see Maccarone et al. 2007; Shih et al. 2010; Dage et al. 2020, for more details).

3 RESULTS

We identified three new GC ULX candidates in NGC 1316, using archival *Chandra* and *HST* observations. The *HST* observations revealed three GC candidates with z and $g - z$, which all had similar sizes. We extracted and fit the X-ray spectra of each source across the six *Chandra* observations. We fit two different single component models to the individual spectra, and also fit models to the combined spectra. Of these, only GCULX2 was able to be fit by a two-component model over a single component model,[3] but in either case the F-test probability was high, meaning that it is not statistically reasonable to add the extra component. Very few GCULXs can be well fitted by a two-component model, only two known sources RZ2109 (Dage et al. 2018) and M87-GCULX1 (Dage et al. 2020) have any evidence for the extra component statistically being a better fit.

Both on the 1 month and the 18 yr time baselines probed, there is no evidence for variations for more than a factor of ∼2, which is consistent with most of the known GC ULXs (Dage et al. 2019a). Only the source in RZ2109 in NGC 4472 (Maccarone et al. 2007), the faded GC ULX identified by Shih et al. (2010) in NGC 1399, and the source SC302 in M87 (Dage et al. 2020) show strong variability on the time-scale of hours. Given that most of the observations are clustered within a single month in 2019, with just one observation occurring in 2001 (see Fig. 3), it is difficult to characterize any long-term variability of these sources.

We also identified 13 X-ray sources coincident with GCs (Table 2), with estimated X-ray luminosities of the order of 10^{38} erg s^{-1}. Given the paucity of the data, we do not perform spectral fits, however, a comprehensive study of similar sources has previously been studied in Irwin, Athey & Bregman (2003).

[3]It is worth noting that GCULX2 has significantly more counts than either of the other two sources.

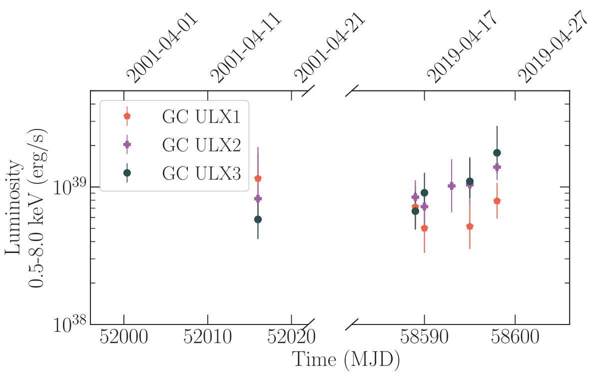

Figure 3. Long-term X-ray luminosity for the three GC ULX sources. Left-hand panel shows the observation from 2001 April (ObsID 2022), and the right-hand panel shows the five observations taken in 2019 April, including upper limits from ObsID 22180 (triangles).

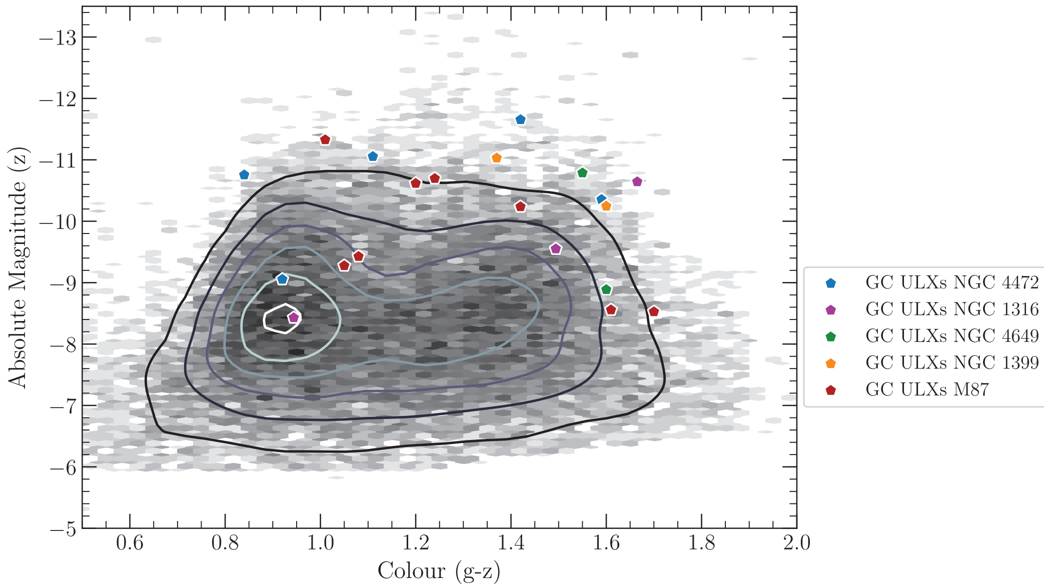

Figure 4. Colour versus magnitude (AB, dereddened) for the GC ULXs, superimposed on the properties of non-ULX hosting clusters in the five galaxies [NGC 1316, NGC 1399, NGC 4472, NGC 4649, and M87, using data from Jordán et al. (2009), Strader et al. (2012b), Peacock et al. (2014), and Jordán et al. (2015)].

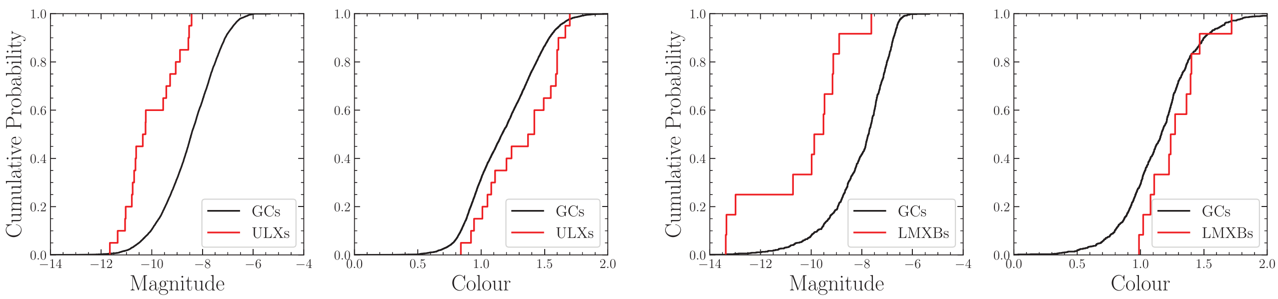

Figure 5. Left: Cumulative distribution functions for z and $g - z$ for the ULX hosting clusters and non-ULX hosting clusters in the five galaxies (NGC 1316, NGC 1399, NGC 4472, NGC 4649, and M87; (Jordán et al. 2009, 2015; Strader et al. 2012b; Peacock et al. 2014; Jordán et al. 2015). Right: Cumulative distribution functions for z and $g - z$ for the NGC 1316 clusters and low X-ray luminosity hosting NGC 1316 clusters.

3.1 Host cluster colour and magnitude

In both Dage et al. (2019a, 2020), we noted that while the ULXs are indeed preferentially hosted by brighter clusters, there is not yet evidence that ULXs hold an affinity for metal rich clusters (unlike the rest of the less-luminous X-ray binary population that shows red clusters outnumbering bluer clusters by three to one as LMXB hosts Kundu, Maccarone & Zepf 2002; Sarazin et al. 2003). Initial studies on a low population of ULX hosting clusters by Maccarone et al. (2011) suggested that it was likely that ULXs are also preferentially hosted by metal rich clusters, however the sample size in this initial study was very small. With the new, larger sample of ULXs hosted by GCs, this question can now be revisited. Nineteen of the GC ULXs have colour and magnitudes measured in the AB magnitude system (see Dage et al. 2019a, 2020, for more). As seen in Fig. 4, the majority of ULXs are not hosted by typical GCs for these galaxies, which certainly highlights the uniqueness of these already-rare sources. We used the Anderson Darling test (Anderson & Darling 1952, 1954) from KSAMPLES[4] to independently compare the optical colour and magnitude distributions of the ULX hosts and other GCs. For the magnitude, the statistic is 22.1 and the significance level is 5.9×10^{-10}. For colour, the statistic value is 3.22 and the significance level is 0.016. The low significance levels imply that the magnitude of the ULX hosts come from very different distributions than the rest of the clusters in these galaxies. However, the tests cannot yet reject the null hypothesis concerning the colour distribution.

NGC 1316 is known to host an intermediate-age population, and therefore the optical colours might not be linearly correlated metallicity for some of NGC 1316's GCs. Infrared colours are known to be more sensitive to metallicity (Kundu & Zepf 2007). To check the metallicities of the NGC 1316 ULX hosting cluster, we also performed photometry in the H band ($F160W$, *HST* observation ib3n03050). GCULX1 was $H = 20.0 \pm 0.2$, GCULX2 was $H = 20.1 \pm 0.4$ and GCULX3 was $H = 21.3 \pm 0.4$. The very red infrared colours ($z - H$) imply that all three ULX hosting clusters of NGC 1316 may be very metal rich. The apparent bluer optical colour of GCULX3 might be because these GCs may be from an intermediate-age population (Goudfrooij et al. 2001b).

Interestingly, while the NGC 1316 clusters that hosted lower luminosity X-ray sources showed a similar preference to be hosted

[4] https://cran.r-project.org/web/packages/kSamples/index.html

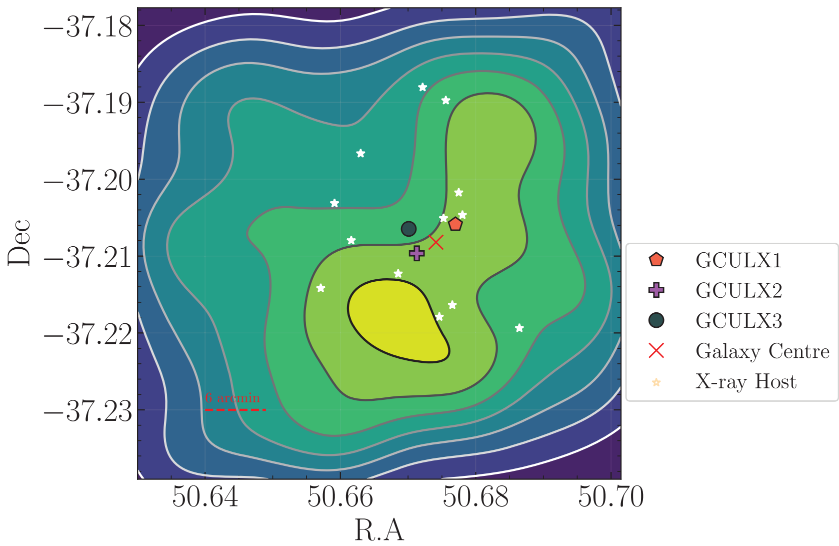

Figure 6. Spatial distribution of GCs in NGC 1316, using GCs identified by Jordán et al. (2015). We caution that the asymmetrical distribution of GCs may be an observational bias caused by obscuration from the dust lanes of the galaxy, although observational evidence for anisotropic GC distribution has been observed in other galaxies such as NGC 4261 (Giordano et al. 2005).

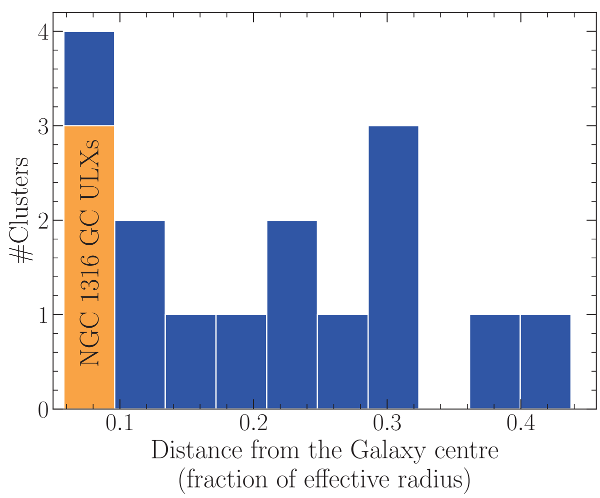

Figure 7. Distance of NGC 1316's X-ray hosting clusters (Table 2) from NGC 1316's galaxy centre as a function of effective radius (taken from the 2MASS catalogue; Skrutskie et al. 2006).

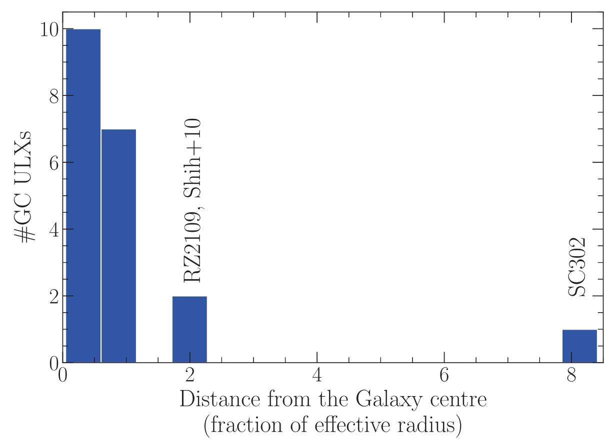

Figure 8. Distance of ULX hosting clusters from their respective galaxy centres as a function of effective radius (taken from the 2MASS catalogue; Skrutskie et al. 2006). The most distant ULX hosts are the NGC 1399 GC ULX observed by Shih et al. (2010), the well-studied and highly variable source RZ2109 in NGC 4472 (Maccarone et al. 2007), and SC302 in M87 (Dage et al. 2020).

by brighter clusters (see Fig. 5). The statistic value comparing the magnitude of the lower luminosity X-ray cluster hosts to the overall NGC 1316 cluster population is 12.6 and the significance level is 4.3×10^{-7}. However, the statistic value for optical colour is 1.52, with a significance level of 0.17, although this is could be due to the smaller sample size.

3.2 Spatial distribution of ULX hosting clusters

As shown in Figs 6 and 7, NGC 1316's GC ULXs are all located near the galaxy centre, with the lower luminosity X-ray hosting clusters more spread out in the system.

The full data set of the now 20 discovered GC ULXs can help address the question of the spatial distribution of the ULX hosting clusters, and whether they are preferentially located near the galaxy centres or outskirts (see Fig. 8). The three farthest ULXs were hosted by clusters over two effective radii from their galaxy centres. Little is known about the nature of the distant NGC 1399 source, as it has not been bright in X-rays since 2003 (Shih et al. 2010), but the NGC 4472 source, RZ2109, is one of the most well-studied GC ULXs, and is thought to be a stellar mass BH accreting from a white dwarf. The host of SC302, the farthest GC ULX identified in M87, by contrast, has optical properties that are ambiguous as to whether the ULX is hosted by a GC or perhaps a stripped nucleus (Dage et al. 2020). In the latter case, this may imply that the accretor of SC302 may be an intermediate-mass BH.

Given the current data, ULXs seem to be overrepresented in the inner regions of the galaxy centre, although we caution that for some galaxies, there may not be complete lists of the GCs, or sufficient X-ray observations to cover the outer regions of all of these galaxies.

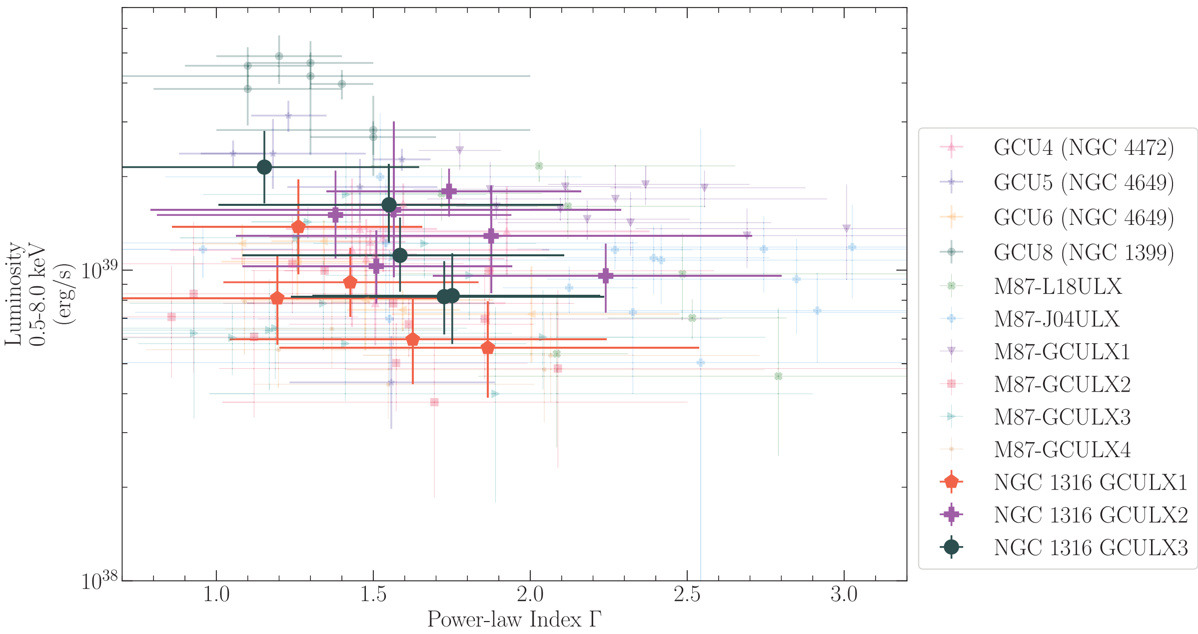

Figure 9. L_X versus Γ for NGC 1316's GC ULX population compared to fit parameters for other known GC ULXs (Dage et al. 2019a, 2020).

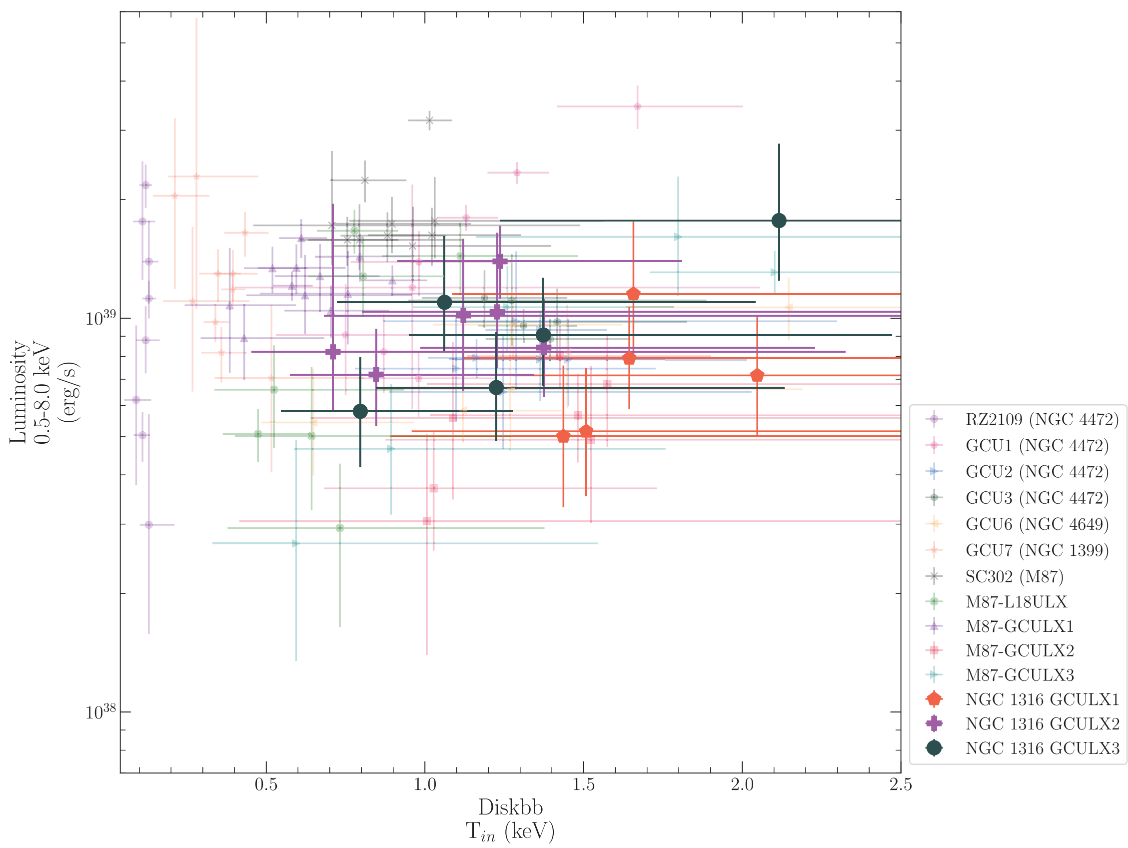

Figure 10. L_X versus $T_{\rm in}$ for NGC 1316's GC ULX population compared to fit parameters for other known GC ULXs (Dage et al. 2018, 2019a, 2020).

3.3 Power-law model fits

Using data from Dage et al. (2018, 2019a, 2020), we can compare the power-law fits of the three NGC 1316 GC ULXs to the previously studied sample. Fig. 9 displays the best-fitting power-law index (Γ) versus the X-ray luminosity (calculated assuming $D = 20.0$ Mpc). The three NGC 1316 GC ULXs seem to follow the same trends as the previously studied sources. Interestingly, GCULX8 in NGC 1399 (where the X-ray luminosity was calculated with $D = 20.0$ Mpc) is still an outlier compared to the rest of the sources, and is intrinsically much brighter, even compared to sources at a comparable distance.

3.4 Blackbody disc model fits

Fig. 10 compares the changes in the measured inner disc temperature ($T_{\rm in}$) to the X-ray luminosity. These sources also appear to follow the same trends as many of the other GC ULXs, where L_X and kT have been established to be correlated in some cases (Dage et al. 2019a). Both RZ2109 in NGC 4472 and GCU7 in NGC 1399 behave differently from the rest of the GC ULXs, with both having low temperatures ($kT < 0.5$ keV), which appear to be independent of the X-ray luminosity. These sources again highlight that the accretion astrophysics is not the same for all of the GC ULXs.

4 CONCLUSIONS

The three new GC ULXs identified in NGC 1316 bring the total known population of GC ULXs to 20. Their behaviour in X-ray is neither as luminous as GCU8 in NGC 1399 nor as strange as RZ2109 in NGC 4472 or GCU7 in NGC 1399. Of the sources studied, the GC ULXs appear to still fall into the same three categories of spectral behaviour: (1) the low kT sources like RZ2109 and GCU7, (2) the 'intermediate' sources with high kT, where both kT and L_X vary, and (3) the sources best fitted by a power-law spectrum.

The intermediate sources in the second group, which have a wide range of best-fitting spectral parameters, may be more comparable to well-studied bright Galactic X-ray binaries (Tetarenko et al. 2016). Many of these sources behave like Galactic X-ray binaries, only with consistently brighter luminosities, or show behaviour similar to sources like GRS 1915 (Tetarenko et al. 2016) (although formed in an older population), which are bright, and only pass the Eddington limit for a 10 solar mass BH for a small fraction of the total observations.

The separate X-ray spectral behaviours of GC ULXs imply that the sources have different combinations of accretor masses/donor stars, and therefore also multiple paths to evolution and formation channels. Given that the X-ray binary formation process in a GC is highly dynamic, and involves multiple interactions with other bodies in the cluster, as well as pair exchanges, it is no surprise that the binary makeup and accretion physics of these systems are also diverse.

Studies of the optical properties of the host clusters show that while the ULXs tend to be more often hosted by luminous clusters, evidence is finally emerging that the host clusters of ULXs are also preferentially redder.

The nature of these sources prompts a number of open questions, in terms of both the high-energy astrophysical phenomena that drive them and the dynamical evolution and formation of these sources. However, given that they are potential tracers of BHs in GCs, they have important implications for the possible origin of merging BHs observed by LIGO, for which BHs in GCs are one of the leading theoretical possibilities (Chatterjee et al. 2017; Rodriguez et al. 2021).

It is currently unclear what properties of the early-type galaxies or their cluster systems will predict whether or not they host ULXs, aside from brighter clusters preferentially hosting ULXs. For instance, Brassington et al. (2010) surveyed bright X-ray sources in NGC 3379, and while three X-ray sources that were found to coincide with GCs were luminous, they were still below the Eddington limit.

NGC 1316 also is home to luminous, but not super-Eddington, X-ray point sources aligned with its GCs. Given the recent merger of the galaxy, and the two different ages of cluster populations, studies of the X-ray luminosity function of the low-mass X-ray binary population are interesting possibilities for a future study.

ACKNOWLEDGEMENTS

This research has made use of data obtained from the *Chandra* Data Archive and the *Chandra* Source Catalog. We also acknowledge use of NASA's Astrophysics Data System and arXiv. KCD and DH acknowledge funding from the Natural Sciences and Engineering Research Council of Canada (NSERC), the Canada Research Chairs (CRC) Program, and the McGill Bob Wares Science Innovation Prospectors Fund. KCD acknowledges fellowship funding from the McGill Space Institute. AK and MBP acknowledge support from NASA through grant number GO-14738 from StSci. SEZ acknowledges support from *Chandra* grants GO9-20080X and AR0-21008B. KCD thanks Carol-Rose Little, Will Clarkson, Eric Koch, Dane Kleiner, and Paolo Serra for their helpful discussion. The following software and packages were used for analysis: CIAO, software provided by the *Chandra* X-ray Center (CXC), HEASOFT obtained from the High Energy Astrophysics Science Archive Research Center (HEASARC), a service of the Astrophysics Science Division at NASA/GSFC and of the Smithsonian Astrophysical Observatory's High Energy Astrophysics Division, SAOIMAGE DS9, developed by Smithsonian Astrophysical Observatory, NUMPY (van der Walt, Colbert & Varoquaux 2011), and MATPLOTLIB (Hunter 2007). This publication makes use of data products from the Two Micron All Sky Survey, which is a joint project of the University of Massachusetts and the Infrared Processing and Analysis Center/California Institute of Technology, funded by the National Aeronautics and Space Administration and the National Science Foundation.

DATA AVAILABILITY

The X-ray data in this article are publicly available through the *Chandra* archive.[5] The optical data are available through MAST.[6]

REFERENCES

Abbott B. P. et al., 2016, ApJ, 833, L1
Allak S., Akyuz A., Aksaker N., Ozdogan Ela M., Avdan S., Soydugan F., 2020, MNRAS, 499, 5682
Anderson T. W., Darling D. A., 1952, Ann. Math. Stat., 23, 193
Anderson T. W., Darling D. A., 1954, J. Am. Stat. Assoc., 49, 765
Arnaud K. A., 1996, in Jacoby G. H., Barnes J., eds, ASP Conf. Ser. Vol. 101, Astronomical Data Analysis Software and Systems V. Astron. Soc. Pac., San Francisco, p. 17
Bachetti M. et al., 2014, Nature, 514, 202
Brassington N. J. et al., 2010, ApJ, 725, 1805
Brightman M. et al., 2018, Nat. Astron., 2, 312
Cash W., 1979, ApJ, 228, 939
Chatterjee S., Rodriguez C. L., Kalogera V., Rasio F. A., 2017, ApJ, 836, L26
Chomiuk L., Strader J., Maccarone T. J., Miller-Jones J. C. A., Heinke C., Noyola E., Seth A. C., Ransom S., 2013, ApJ, 777, 69
Dage K. C., Zepf S. E., Bahramian A., Kundu A., Maccarone T. J., Peacock M. B., 2018, ApJ, 862, 108
Dage K. C., Zepf S. E., Peacock M. B., Bahramian A., Noroozi O., Kundu A., Maccarone T. J., 2019a, MNRAS, 485, 1694
Dage K. C., Zepf S. E., Thygesen E., Bahramian A., Kundu A., Maccarone T. J., Peacock M. B., Strader J., 2020, MNRAS, 497, 596
Dage K. C. et al., 2019b, MNRAS, 489, 4783

[5]https://cda.harvard.edu/chaser/
[6]https://archive.stsci.edu/

Dickey J. M., Lockman F. J., 1990, ARA&A, 28, 215
Giersz M., Askar A., Wang L., Hypki A., Leveque A., Spurzem R., 2019, MNRAS, 487, 2412
Giesers B. et al., 2018, MNRAS, 475, L15
Giesers B. et al., 2019, A&A, 632, A3
Giordano L., Cortese L., Trinchieri G., Wolter A., Colpi M., Gavazzi G., Mayer L., 2005, ApJ, 634, 272
Goudfrooij P., Alonso M. V., Maraston C., Minniti D., 2001b, MNRAS, 328, 237
Goudfrooij P., Mack J., Kissler-Patig M., Meylan G., Minniti D., 2001a, MNRAS, 322, 643
Hu C.-P., Ueda Y., Enoto T., 2021, ApJ, 909, 5
Hunter J. D., 2007, Comput. Sci. Eng., 9, 90
Irwin J. A., Athey A. E., Bregman J. N., 2003, ApJ, 587, 356
Irwin J. A., Bregman J. N., Athey A. E., 2004, ApJ, 601, L143
Irwin J. A., Brink T. G., Bregman J. N., Roberts T. P., 2010, ApJ, 712, L1
Irwin J. A. et al., 2016, Nature, 538, 356
Jordán A., Peng E. W., Blakeslee J. P., Cote P., Eyheramendy S., Ferrarese L., 2015, ApJS, 221, 13
Jordán A. et al., 2009, ApJS, 180, 54
Kim D.-W., Fabbiano G., 2003, ApJ, 586, 826
Kleiner D. et al., 2021, A&A, 648, A32
Kremer K., Chatterjee S., Ye C. S., Rodriguez C. L., Rasio F. A., 2019, ApJ, 871, 38
Krist J. E., Hook R. N., Stoehr F., 2011, in Kahan M. A., ed., Proc. SPIE Conf. Ser. Vol. 8127, Optical Modeling and Performance Predictions V. SPIE, Bellingham, p. 81270J
Kundu A., Maccarone T. J., Zepf S. E., 2002, ApJ, 574, L5
Kundu A., Zepf S. E., 2007, ApJ, 660, L109
Larsen S. S., 1999, A&AS, 139, 393
Maccarone T. J., Kundu A., Zepf S. E., Rhode K. L., 2007, Nature, 445, 183
Maccarone T. J., Kundu A., Zepf S. E., Rhode K. L., 2011, MNRAS, 410, 1655
Miller-Jones J. C. A. et al., 2015, MNRAS, 453, 3918
Peacock M. B., Zepf S. E., Maccarone T. J., Kundu A., Gonzalez A. H., Lehmer B. D., Maraston C., 2014, ApJ, 784, 162
Peacock M. B. et al., 2012, ApJ, 759, 126
Roberts T. P. et al., 2012, ApJ, 760, 135
Rodriguez C. L., Kremer K., Chatterjee S., Fragione G., Loeb A., Rasio F. A., Weatherford N. C., Ye C. S., 2021, AAS, 5, 19
Rodriguez C. L., Zevin M., Amaro-Seoane P., Chatterjee S., Kremer K., Rasio F. A., Ye C. S., 2019, Phys. Rev. D, 100, 043027
Sarazin C. L., Kundu A., Irwin J. A., Sivakoff G. R., Blanton E. L., Rand all S. W., 2003, ApJ, 595, 743
Shih I. C., Kundu A., Maccarone T. J., Zepf S. E., Joseph T. D., 2010, ApJ, 721, 323
Shishkovsky L. et al., 2018, ApJ, 855, 55
Sivakoff G. R., Sarazin C. L., Jordán A., 2005, ApJ, 624, L17
Skrutskie M. F. et al., 2006, AJ, 131, 1163
Spitzer L, 1969, ApJ, 158L, 139
Steele M. M., Zepf S. E., Kundu A., Maccarone T. J., Rhode K. L., Salzer J. J., 2011, ApJ, 739, 95
Steele M. M., Zepf S. E., Maccarone T. J., Kundu A., Rhode K. L., Salzer J. J., 2014, ApJ, 785, 147
Stetson P. B., 1987, PASP, 99, 191
Strader J., Chomiuk L., Maccarone T. J., Miller-Jones J. C. A., Seth A. C., 2012a, Nature, 490, 71
Strader J. et al., 2012b, ApJ, 760, 87
Swartz D. A., Ghosh K. K., Tennant A. F., Wu K., 2004, ApJS, 154, 519
Tetarenko B. E., Sivakoff G. R., Heinke C. O., Gladstone J. C., 2016, ApJS, 222, 15
van der Walt S., Colbert S. C., Varoquaux G., 2011, Comput. Sci. Eng., 13, 22
Wiktorowicz G., Lasota J.-P., Belczynski K., Lu Y., Liu J., Iłkiewicz K., 2021, preprint (arXiv:2103.02026)
Ye C. S., Fong W.-f., Kremer K., Rodriguez C. L., Chatterjee S., Fragione G., Rasio F. A., 2020, ApJ, 888, L10
Zepf S. E. et al., 2008, ApJ, 683, L139

This paper has been typeset from a TEX/LATEX file prepared by the author.